Scanned Probe Imaging of Quantum Dots inside InAs Nanowires

Ania C. Bleszynski,[†] Floris A. Zwanenburg,[‡] R. M. Westervelt,*,[†] Aarnoud L. Roest,[§] Erik P. A. M. Bakkers,[§] and Leo P. Kouwenhoven[‡]

Department of Physics and School of Engineering and Applied Sciences, Harvard University, Cambridge, Massachusetts 02138, Kavli Institute of Nanoscience, Delft University of Technology, Delft, The Netherlands, and Philips Research Laboratories, Eindhoven, The Netherlands

ABSTRACT

We show how a scanning probe microscope (SPM) can be used to image electron flow through InAs nanowires, elucidating the physics of nanowire devices on a local scale. A charged SPM tip is used as a movable gate. Images of nanowire conductance versus tip position spatially map the conductance of InAs nanowires at liquid-He temperatures. Plots of conductance versus backgate voltage without the tip present show complex patterns of Coulomb-blockade peaks. Images of nanowire conductance identify their source as multiple quantum dots formed by disorder along the nanowire—each dot is surrounded by a series of concentric rings corresponding to Coulomb blockade peaks. An SPM image locates the dots and provides information about their size. In this way, SPM images can be used to understand the features that control transport through nanowires. The nanowires were grown from metal catalyst particles and have diameters ~80 nm and lengths 2–3 μm.

An explosion in research activity on semiconducting nanowires has occurred in the past decade.[1–3] The ability to control the dimensions and composition of nanowire devices shows great promise for nanoelectronics, nanophotonics, and quantum information processing. Quantum effects are naturally important due to their small size, opening new possibilities for quantum devices.

InAs nanowires are a particularly attractive system for several reasons. InAs has a large g-factor, making it useful for spintronics and quantum information processing. Its large bulk exciton Bohr radius $a_B = 34$ nm is comparable to the radius of nanowires studied in this paper, producing quantum confinement. While some semiconductors are known to have a surface depletion layer, the surface of InAs is known to have a charge accumulation layer. As a result, very small radius nanowires are not depleted of electrons, and one can make Schottky-barrier-free contacts to metallic leads.

Recent achievements in the field of semiconducting nanowires including single-electron control,[4–6] high-performance field-effect transistors,[7] and proximity-induced superconductivity.[8,9] Progress requires an understanding of where the electrons are along the nanowire and how they flow through it. Standard transport measurements provide information about the conductance of the whole length of the nanowire[4–6] but do not provide detailed spatial information.

Scanning probe microscope (SPM) imaging allows one to probe the motion of electrons along the nanowire locally, with high spatial resolution, and to modify the potential profile to allow or block electron transport. Cooled scanned probe microscopes have proven to be powerful tools for imaging and controlling electron flow in nanoscale systems including carbon nanotubes, a two-dimensional electron gas, and GaAs quantum dots.[10–16] Imaging techniques for nanowires are just being developed.[17,18]

In this Letter we present conductance images of InAs nanowires obtained with a liquid-He-cooled SPM. Plots of nanowire conductance G versus backgate voltage V_{bg} without the tip present show complex patterns of Coulomb blockade peaks with uneven spacings and heights. SPM images of nanowire conductance, using the tip as a movable gate, show the pattern of peaks is produced by multiple quantum dots located along the InAs nanowire, accidentally produced by disorder. Each dot is surrounded by a set of concentric rings of high conductance corresponding to Coulomb blockade conductance peaks.[12] The spacing and intensity of the rings about a dot provide information about the dot size and tunneling rate. The rings from nearby dots overlap. By using the tip as a movable gate, we can tune the charge state of each dot individually. These results show how a cooled SPM

---
* Corresponding author: westervelt@deas.harvard.edu.
† Harvard University.
‡ Delft University of Technology.
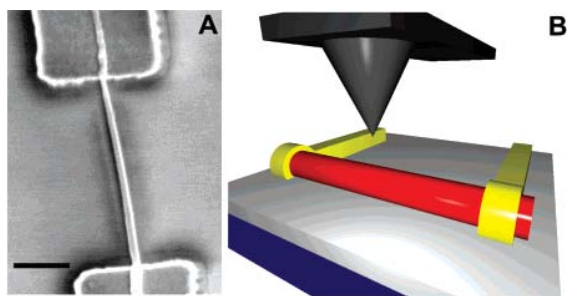§ Philips Research Laboratories.

Figure 1. (A) SEM photo of an InAs nanowire (device D1) contacted with Ti/Al electrodes. (The slight kink in the wire at the top contact, due to an atomic force microscope (AFM) tip crash, occurred after the data presented in this paper was obtained.) The scale bar is 500 nm long. (B) Imaging schematic. A charged AFM tip is scanned ∼100 nm above the contacted InAs nanowire. Nanowire conductance as a function of lateral tip position is recorded to form an image. The wire lies atop a conducting Si substrate with a 250 nm thick SiO_2 capping layer.

can be a powerful diagnostic tool for the development of nanowire devices.

The InAs nanowires were grown in a catalytic process from small gold seed particles using metal−organic vapor-phase epitaxy.[19] The nanowires have diameters ∼80 nm and lengths ∼2−3 μm. After growth, the InAs nanowires are transferred onto a conducting p+ silicon substrate capped with a 250 nm thick SiO_2 insulating layer. The silicon substrate acts as a backgate that can tune the number of charge carriers in the wire through an applied backgate voltage V_{bg}. Electron beam lithography is used to define electrodes ∼2 μm apart, and 110 nm of Ti/Al is subsequently deposited to form the contacts. Figure 1A shows a scanning electron microscopy (SEM) picture of a contacted InAs wire.

A home-built liquid-He-cooled SPM is used to image electrical conduction through the nanowires. As schemati-

cally shown in Figure 1B, an image is obtained by scanning a conducting SPM tip across a plane above the nanowire and recording the nanowire conductance G versus tip position with fixed V_{tip} and V_{bg}.[12] The conducting tip gates the nanowire *locally*, whereas the backgate gates the nanowire *globally*. The tip voltage V_{tip} creates a dip or peak in the electron density below. For an open nanowire, one can image electron flow by using the tip to scatter electrons, thereby changing G. However, for a quantum dot in the Coulomb blockade regime, a different pattern is observed. An image of a dot shows a series of concentric rings corresponding to Coulomb blockade conductance peaks that occur as electrons are added to the dot. This Coulomb blockade imaging technique has been used to image multielectron quantum dots formed in carbon nanotubes[11] and a one-electron GaAs quantum dot.[12]

Parts A and B of Figure 2 show plots of nanowire conductance G versus backgate voltage V_{bg} for two InAs nanowire devices, D1 and D2; the nanowires are near pinchoff with $G \ll e^2/h$. Each plot shows an irregular series of peaks with variable spacing and amplitude similar to Coulomb blockade oscillations for multiple quantum dots in series.[20−22] The low conductance and the existence of complex patterns of peaks show the InAs nanowires are not spatially uniform. Without additional information, it is difficult to identify the source of these irregular oscillations.

The SPM conductance images in parts C and D of Figure 2 show the presence of multiple quantum dots located along each nanowire. Nested conductance rings occur about three positions along nanowire D1 in Figure 2C and about two positions along nanowire D2 in Figure 2D. Each ring corresponds to a Coulomb conductance peak of the quantum dot at the ring's center as electrons are added or removed
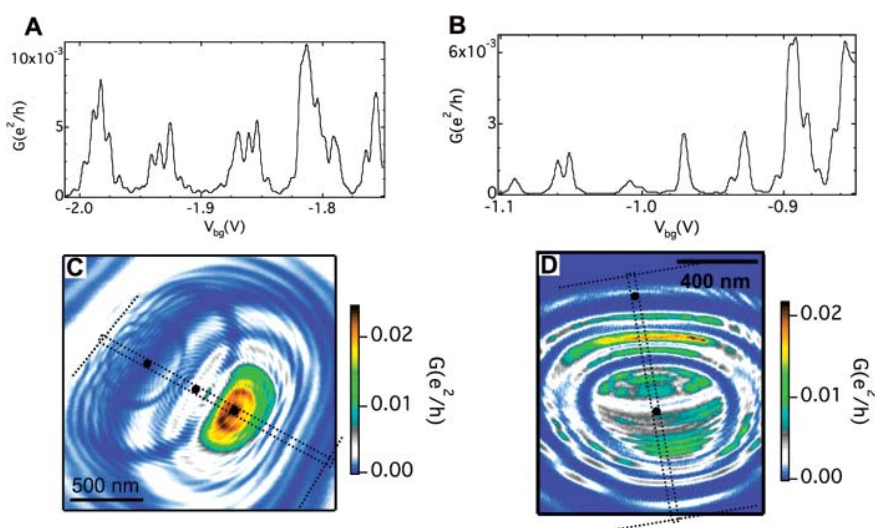

Figure 2. InAs nanowire transport measurements and corresponding images that spatially illuminate the behavior. (A, B) Nanowire conductance G vs backgate voltage V_{bg} for devices D1 and D2, respectively. The plots show a complex pattern of Coulomb blockade conductance peaks characteristic of multiple quantum dots in series. From these plots, it is difficult to determine the number and locations of the dots in each wire. (C, D) SPM images of devices D1 and D2, respectively, that display G vs position of a charged SPM tip scanned along a plane 100 nm above the nanowire. Concentric rings of high conductance, corresponding to Coulomb blockade peaks, are centered on quantum dots in the nanowire. (C) shows three sets of concentric rings identify three quantum dots whose positions are marked by black dots. (D) reveals rings surrounding two quantum dots in the nanowire. Dotted lines denote the outline of the wire and the electrical contacts.
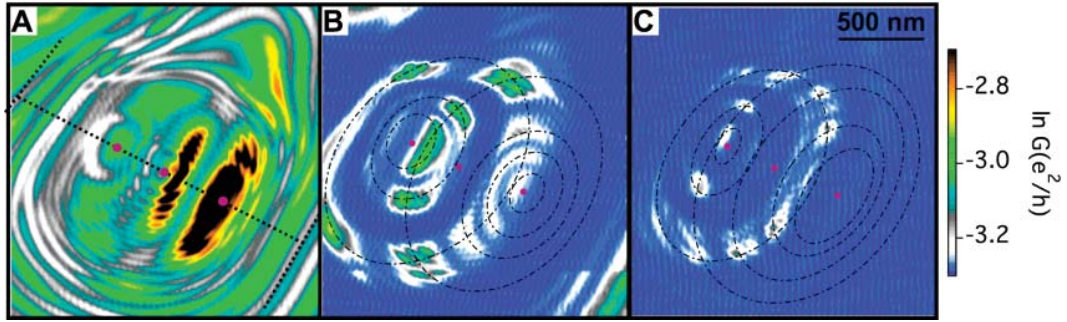
Figure 3. SPM images of conductance G for device D1 showing the interaction of Coulomb blockade rings from the three quantum dots in the nanowire. Pink dots mark the dot locations, and dashed lines show outlines of the nanowire and contacts in (A). The images were recorded with $V_{tip} = 0$ V and backgate voltages (A) $V_{bg} = -1.94$ V, (B) -2.05 V, and (C) -2.12 V. As V_{bg} is made more negative, conductance occurs only near the intersection of rings from different dots, where each dot is on a Coulomb blockade conductance peak. Elliptical dash-dotted rings in (B) and (C) show the location of rings in (A) from the two outermost dots. The expected rings for the middle dot have not been shown, because they are so closely spaced that their inclusion would clutter the image.
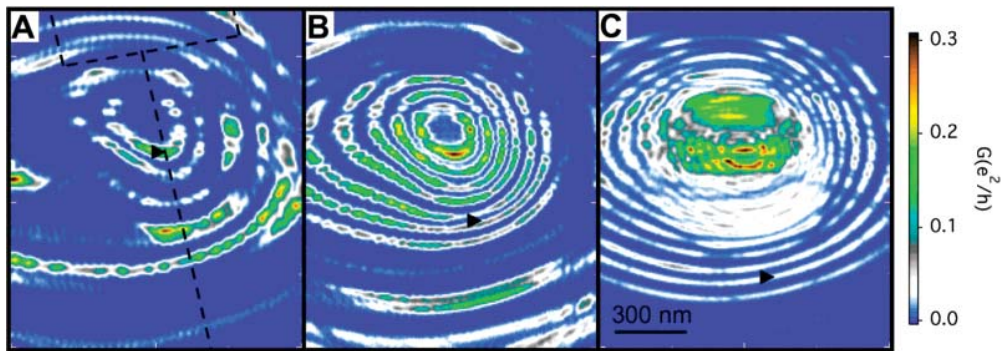

Figure 4. Evolution of SPM images of device D2 with tip voltages: (A) $V_{tip} = 0.48$ V, (B) 0.90 V, and (C) 1.44 V. The wire and top contact are denoted with dashed lines in (A). Coulomb blockade rings surround a quantum dot in the upper half of the image. As V_{tip} increases, the rings expand outward in size and become more closely spaced. The black triangle tracks one Coulomb peak, demonstrating how the size of the rings grows with tip voltage.

by the SPM tip.[11,12] The charge induced by the tip on a single dot is

$$q_{ind}(r_{t-d}, V_{t-d}) = C_{t-d}(r_{t-d}) * V_{t-d} \qquad (1)$$

where r_{t-d} is the distance between the tip and the dot, C_{t-d} is the capacitance between the tip and the dot (assuming a conducting dot with a fixed geometry), and V_{t-d} is the voltage difference between tip and dot, including effects of the contact potential and the dot's capacitance to ground. Because C_{t-d} changes with tip position, the induced charge q_{ind} can be controlled either by the tip voltage V_{tip} or by the tip position r_{t-d}. If one were to plot G versus r_{t-d}, a conductance peak would occur every time the charge in the dot changes by one electron. In images, the conductance peaks take the form of closed rings centered on the dot that are contours of constant tip-to-dot capacitive coupling C_{t-d}. When the tip is between two rings, the dot charge remains constant at an integer multiple of the electron charge e.

The images in parts C and D of Figure 2 show that the complex conductance plots in parts A and B of Figure 2 were caused by multiple quantum dots in series. In Figure 2C, three sets of concentric rings indicate the presence of three quantum dots at locations indicated by the black dots

superimposed on the image. The rings surrounding the middle dot in D1 are more closely spaced than those surrounding the other two dots, indicating that the center dot is larger. In Figure 2D, two sets of concentric rings indicate the presence of two quantum dots, whose locations are again marked by black dots. In both parts C and D of Figure 2, the rings are elongated along an axis perpendicular to the wire due to a slight screening of the tip by the metal contacts. Formation of the quantum dots is accidental, presumably due to local potential fluctuations or defects in the nanowires.

The SPM images together with plots of G versus V_{bg} allow us to estimate the sizes of the quantum dots located along the nanowire. We use a simple model in which the capacitance C_{bg} between the dot and the backgate is given by the capacitance of a cylindrical nanowire segment[23] of radius $r = 40$ nm and length L located at a height z above the backgate $C_{bg} = 2\pi\epsilon_r\epsilon_0 L/\ln(2z/r)$; here ϵ_0 is the permittivity of a vacuum, $z = 250$ nm is the thickness of the insulating SiO_2 layer, and $\epsilon_r = 2.0$ is the average dielectric constant including both the SiO_2 layer and the gap between the nanowire and SiO_2 layer away from the line where they touch. The length L of a given dot can be estimated from the period of its Coulomb blockade conductance oscillation

versus V_{bg}. For Figure 2A this is possible for the rapid oscillation. This rapid oscillation corresponds to the closely spaced rings about the middle dot in the image Figure 2C; the ring spacing for the other dots is larger. Comparing the backgate voltage period with the ring spacing for a given dot calibrates the image for all of the dots shown, so that the ring spacing for another dot can be used to estimate its length L, even if its conductance oscillation cannot be picked out of the G versus V_{bg} conductance plot. Using this procedure, we found the lengths of the three dots from left to right in Figure 2C for sample D1 to be $L = 63$, 520, and 140 nm, and the lengths of the two dots from top to bottom in Figure 2D for sample D2 to be $L = 400$ and 122 nm. The dot lengths vary, and some dots are longer than their diameter, as one might expect for accidental dots.

Using the SPM tip as a movable gate allows us to control the charge on one dot in a nanowire that contains many dots, like the devices shown here. The movable gate technique has a great advantage over static gating techniques for the manipulation of quantum dots in nanowires: The movable gate allows one to image and locate the position of one or more quantum dots along a nanowire. In addition, the SPM tip can be used to address an individual dot in a nanowire that contains multiple dots. Doing this can be difficult using lithographically defined gates if the dot locations are unknown or if the spacing between two dots is smaller than the lithographic resolution.

The images in Figure 3 show how the nanowire conductance is pinched off by a negative backgate voltage to produce Coulomb conductance peak patterns characteristic of quantum dots in series.[20] The electron density is reduced everywhere in the nanowire, producing effectively higher barriers. A series of SPM images of device D1 are shown in parts A–C of Figure 3 for $V_{\text{bg}} = -1.94$, -2.05, and -2.12 V, respectively. The small pink dots in Figure 3 show quantum dot locations, and the dashed ellipses in panels B and C of Figure 3 show the location of the rings for the two outer dots from Figure 3A. As the nanowire is depleted, conductance only occurs when all three dots are on a Coulomb blockade peak; this occurs at the intersections of conductance rings from different dots. Clearly seen in Figure 3C, this peaks at the intersection of conductance rings from different dots is the expected pattern for multiple quantum dots in series with negligible coupling between them.[20]

The SPM images of device D2 in Figure 4 show how the Coulomb blockade rings from a given dot evolve as the tip voltage is increased from $V_{\text{tip}} = 0.48$ to 1.44 V while keeping V_{bg} constant: the rings move radially outward, and their spacing decreases. In these images, a dominant set of rings is centered on the quantum dot in the upper half of the image. We can track the motion of an individual ring by taking a series of images with small increments in V_{tip} (see Supporting Information). A subset of these images is shown in Figure 4, where a superimposed black triangle is used to indicate the location of a particular ring. The radius grows as V_{tip} is increased, because the positive tip pulls more electrons onto the dot. It is difficult to estimate the absolute number of electrons, because the dot contains many electrons and we cannot deplete the number to zero. In addition, the rings become more closely spaced as V_{tip} is increased, because the induced charge on the dot increases, in proportion to V_{tip}. So a smaller change in tip position and tip-to-dot capacitance $C_{\text{t-d}}$ is needed to add or remove one electron.

Supporting Information Available: A series of cooled scanning probe microscope images of nanowire device D2 taken as the tip voltage varied from 0.48 to 1.44 V. This material is available free of charge via the Internet at http://pubs.acs.org.

References

(1) Lieber, C. M. *MRS Bull.* **2003**, *28*, 486.
(2) Yang, P. *MRS Bull.* **2005**, *30*, 85.
(3) Samuelson, L.; Thelander, C.; Bjork, M. T.; Borgstrom, M.; Deppert, K.; Dick, K. A.; Hansen, A. E.; Martensson, T.; Panev, N.; Persson, A. I.; Seifert, W.; Skold, N.; Larsson, M. W.; Wallenberg, L. R. *Physica E: Low-dimens. Syst. Nanostruct.* **2005**, *25*, 313.
(4) Zhong, Z.; Fang, Y; Lu, W.; Lieber, C. M. *Nano Lett.* **2005**, *5*, 1143.
(5) De Franceschi, S.; van Dam, J. A.; Bakkers, E. P. A. M.; Feiner, L. F.; Gurevich, L.; Kouwenhoven, L. P. *Appl. Phys. Lett.* **2003**, *83*, 344.
(6) Bjork, M. T.; Thelander, C.; Hansen, A. E.; Jensen, L. E.; Larsson, M. W.; Wallenberg, L. R.; Samuelson, L. *Nano Lett.* **2004**, *4*, 1621.
(7) Xiang, J.; Lu, W.; Hu, Y.; Wu, Y.; Yan, H.; Lieber, C. M. *Nature* **2006**, *441*, 489.
(8) Doh, Y.; Van dam, J. A.; Roest, A. L.; Bakkers, E. P. A. M.; Kouwenhoven, L. P.; De Franceschi, S. *Science* **2005**, *309*, 272.
(9) Xiang, J.; Vidan, A.; Tinkham, M.; Westervelt, R. M.; Lieber, C. M.; *Nat. Nanotechnol.* **2006**, 1, 208.
(10) Topinka, M. A.; Westervelt, R. M.; Heller, E. J. *Phys. Today* **2003**, December, 47.
(11) Woodside, M. T.; McEuen, P. L. *Science* **2002**, *296*, 1098.
(12) Fallahi, P.; Bleszynski, A. C.; Westervelt, R. M.; Huang, J.; Walls, J. D.; Heller, E. J.; Hanson, M.; Gossard, A. C. *Nano Lett.* **2005**, *5*, 223.
(13) Pioda, A.; Kicin, S.; Ihn, T.; Sigrist, M.; Fuhrer, A.; Ensslin, K.; Weichselbaum, A.; Ulloa, S. E.; M. Reinwald, M.; Wegscheider, W. *Phys. Rev. Lett.* **2004**, *93*, 216801.
(14) Bockrath, M.; Liang, W.; Bozovic, D.; Hafner, J. H.; Lieber, C. M.; Tinkham, M.; Park, H. *Science* **2001**, *291*, 283.
(15) Tans, S. J.; Dekker, C. *Nature* **2000**, *404*, 834.
(16) Zhitenev, N. B.; Fulton, T. A.; Yacoby, A.; Hess, H. F.; Pfeiffer, L. N.; West, K. W. *Nature* **2000**, *404*, 473.
(17) Ahn, Y.; Dunning, J.; Park, J. *Nano Lett.* **2005**, *5*, 1367.
(18) Gu, Y.; Kwak, E.-S.; Lensch, J. L.; Allen, J. E.; Odom, T. W.; Lauhon, L. J. *Appl. Phys. Lett.* **2005**, *87*, 043111.
(19) Bakkers, E. P. A. M.; Van Dam, J. A.; De Franceschi, S.; Kouwenhoven, L. P.; Kaiser, M.; Verheijen, M.; Wondergem, H.; Van Der, Sluis, P. *Nat. Mater.* **2004**, *3*, 769.
(20) Waugh, F. R.; Berry, M. J.; Mar, D. J.; Westervelt, R. M.; Campman, K. L.; Gossard, A. C. *Phys. Rev. Lett.* **1995**, *75*, 705.
(21) Kouwenhoven, L. P.; Marcus, C. M.; McEuen, P. L.; Tarucha, S.; Westervelt, R. M.; Wingreen, N. S. In *Mesoscopic Electron Transport*; Sohn, L. L., Kouwenhoven, L. P., Schon, G., Eds.; Kluwer: Dordrecht, 1997.
(22) Ruzin, I. M.; Chandresekar, V.; Levin, E. I.; Glazman, L. I. *Phys. Rev. B* **1992**, *45*, 13469.
(23) Yao, Zhen; Dekker, Cees; Avouris, Phaedon *Topics in Applied Physics*; Dresselhaus, M. S., Dresselhaus, G., Avouris, Ph., Eds., Springer-Verlag: Berlin, 2001; Vol. 80, pp 147−171.